Theoretical Study of the Thermal Dissociation Mechanism of AH_4 (A = Si, Ge, Sn, Pb)

ARTICLE *in* CHEMINFORM · APRIL 2004

Impact Factor: 0.74 · DOI: 10.1021/jp049460v

3 AUTHORS, INCLUDING:

Alberto Vela
Center for Research and Advanced Studies of…
126 PUBLICATIONS **2,519** CITATIONS

Theoretical Study of the Thermal Dissociation Mechanism of AH_4 (A = Si, Ge, Sn, Pb)

Gabriel Merino,[†] Sigfrido Escalante,[‡] and Alberto Vela*

Departamento de Química, Centro de Investigación y de Estudios Avanzados, A. P. 14-740, México D.F. 07000, México

Received: February 5, 2004; In Final Form: March 18, 2004

Structural, energetic, and vibrational data for the species involved in the unimolecular dissociation reaction $AH_4 \rightarrow AH_2 + H_2$, A = Si, Ge, Sn, Pb, are presented. For all the hydrides considered and independently of the theoretical methodology, a set of intermediates were detected. It is shown that a group of four normal modes, two from the product AH_2 and the other two from the intermediate, can be used to assign some experimental bands in the infrared spectra. The stability of the molecular complexes is explained as a result of a small transfer of electrons from the hydrogen molecule to the dihydride.

I. Introduction

The steady development of the microelectronic industry in the last three decades requires a deeper understanding of some of the chemical and physical processes involved. One of them is the chemical vapor deposition (CVD) of amorphous silicon and germanium films on silicon crystals that is done with silane and germane as the source atoms.[1−5] In this process, a complicated and not completely well understood mechanism produces the final deposition of the atoms on the surface. For the thermal decomposition of silane, SiH_4, it has been proposed that the reaction follows a mechanism with two predissociations where silylene, SiH_2, is involved. For the general case, the reactions are

$$AH_4 \rightarrow AH_2 + H_2 \quad (1)$$

$$AH_2 \rightarrow A + H_2 \quad (2)$$

where A = Si, Ge, Sn, Pb.

Several authors have calculated the barrier for hydrogen insertion into AH_2,[6−11] the reverse of reaction 1. In the case of silane, the barrier has been determined experimentally.[12] It has been shown, experimentally and theoretically, that the photodissociation of germylene proceeds through a pathway where excited states are involved. However, despite the many efforts that have been made to detect all the species involved in the mechanism, some intermediate steps are still unresolved.[13]

In the case of lead, for many years it was believed the plumbane, PbH_4, was a nonexisting compound.[14] However, recent spectroscopic evidence suggests that plumbane is stable enough to be detected in the gas phase.[15,16] In a series of works involving A_mH_n (A = Si−Pb, m = 1, 2, and n = 2, 3, 4, 6) compounds,[16−19] Andrews and co-workers reported evidence supporting the existence of plumbane. Even though the analysis of Andrews and collaborators was very detailed and complete, some bands of the infrared spectra were not fully assigned. Thus, further work is necessary to fully understand which chemical structures are participating in the thermal dissociation reactions of group 14 hydrides.

A very important issue that has been clearly considered by some authors,[6,7,20] and doubtfully by others,[16−19] is the possible existence of an intermediate in the unimolecular dissociation of AH_4. Along this vein, it is worth noting that Kapp et al. found, and characterized as minima, a set of stationary points on the potential energy surface (PES) of the cations AH_3^+ (A = Si−Pb) that can be described as weak complexes of the type $AH^+ \cdot\cdot H_2$.[21]

The studies mentioned above underline the importance of performing an exhaustive and detailed theoretical analysis regarding the existence of intermediates in the unimolecular dissociation of group 14 tetrahydrides, which constitutes the main aim of the present work.

II. Computational Details

Second-order Møller−Plesset (MP2),[22] coupled Cluster including single, double, and noniteratively triple excitations (CCSD(T)),[23−27] and density functional calculations with the hybrid exchange-correlation energy functional B3LYP[28−30] were done in conjunction with two different effective core potentials (ECPs): LanL2DZ,[31] with the corresponding split-valence basis set augmented by p and d polarization functions,[32] and the Stuttgart−Dresden ECPs (SDD)[33] with an extra d-polarization function for the valence basis set for Ge, Sn, and Pb, from Huzinaga.[34] In all cases, the basis set used for H was a (5s,1p) → [3s,1p] contraction from Dunning and Hay.[35] For the silicon and germanium hydrides, all-electron calculations were also performed with the augmented cc-pVTZ (aug-cc-pVTZ) basis set.[36] We will refer to the methods by an acronym followed by I for aug-cc-pVTZ, II for LanL2DZ+dp ECPs, and III for Stuttgart ECPs. Nonrelativistic calculations for Pb compounds were also done with B3LYP/SDD to evaluate the magnitude of relativistic effects in the trends of several properties. Geometry optimizations were done without symmetry constraints. The ground states of the carbene-type hydrides AH_2, for A = Si−Pb, are singlets, in contrast to methylene which has a triplet ground-state multiplicity. Therefore, all molecular systems considered were in their $^1A_1$ ground electronic state. All the stationary points found on the PES were characterized by a harmonic vibrational frequency analysis. The B3LYP, MP2, and

* Address correspondence to this author. E-mail: avela@mail.cinvestav.mx. Fax: +52-55/5747-7113.

† Present address: Technische Universität Dresden, Institut für Physikalische Chemie und Elektrochemie, D-01062 Dresden; Germany.

‡ On sabbatical leave from the Departamento de Química Inorgánica y Nuclear, Facultad de Química, UNAM, México.

10.1021/jp049460v CCC: $27.50
Published on Web 04/29/2004

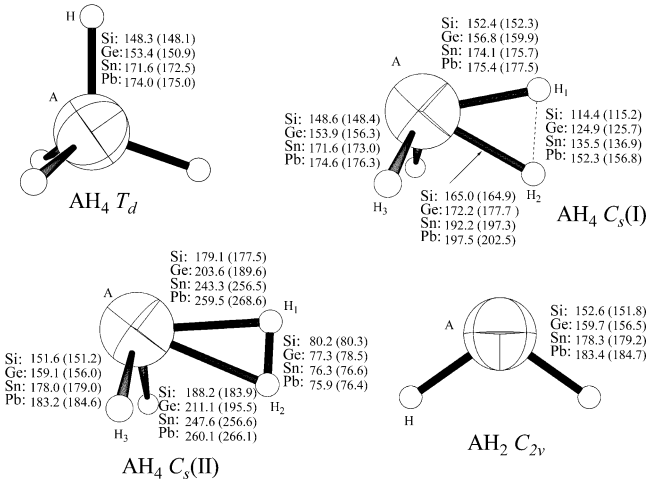

Figure 1. B3LYP and, in parentheses, CCSD(T), optimized geometries of the stationary points of group 14 tetrahydrides.

CCSD(T) zero-point energies (ZPE) were scaled by a factor of 0.9806, 0.9661, and 0.95, respectively.[37,38] To verify that the transition states connect the appropriate minima, a set of intrinsic reaction coordinate (IRC)[39,40] calculations with the B3LYP hybrid functional and the LanL2DZ+dp ECP were carried out. All calculations were done with Gaussian 98.[41] The molecular orbitals were plotted with the molecular graphics package MOLEKEL.[42,43]

III. Geometries and Energetics

The chemical species calculated in this work are those involved in the thermal dissociation reaction of a tetrahydride of a group 14 element

$$AH_4,\ T_d \rightarrow AH_4^*,\ C_s(I) \rightarrow AH_4,\ C_s(II) \rightarrow AH_2,\ C_{2v} + H_2 \quad (3)$$

The stationary points found on the PES of this reaction are depicted in Figure 1, and they correspond to a T_d minimum, a C_s(I) transition state, a C_s(II) minimum, and the products of the reaction.

TABLE 1: Bond Distances (in pm) and Bond Angles (in deg) for AH_n Compounds (A = Si, Ge, Sn, Pb, n = 2, 4)

		AH_4, T_d		AH_2, C_{2v}	
A	method	A−H	H−H	A−H	H−A−H
Si	B3LYP/I	148.3		152.6	91.6
	MP2/I	147.5		151.1	91.8
	CCSD(T)/I	148.1		151.8	91.9
	B3LYP/II	148.2		152.2	91.9
	B3LYP/III	149.4		154.4	90.8
	MP2/II	148.3		151.9	92.1
	CCSD(T)/II	148.9		152.9	92.0
	experiment[a,b]	147.5		151.6	92.8
Ge	B3LYP/I	153.4		159.7	90.9
	MP2/I	149.9		155.2	91.4
	CCSD(T)/I	150.9		156.5	91.4
	B3LYP/II	154.7		160.7	90.9
	B3LYP/III	154.6		161.8	90.6
	MP2/II	154.8		160.4	90.9
	CCSD(T)/II	155.6		161.6	90.8
	experiment[a,b]	152.0		159.1(7)	91.2(8)
Sn	B3LYP/II	171.6		178.3	90.7
	B3LYP/III	171.8		179.4	90.4
	MP2/II	171.7		177.9	90.9
	CCSD(T)/II	172.5		179.2	90.9
	experiment[a]	170.0			
Pb	B3LYP/II	174.0		183.4	90.4
	B3LYP/III	174.7		185.0	90.8
	MP2/II	173.9		183.3	90.3
	CCSD(T)/II	175.0		184.7	90.3
	experiment[c]	173.0[d]			
H_2	B3LYP/I		74.3		
	MP2/I		73.7		
	CCSD(T)/I		74.3		
	B3LYP/II		74.9		
	MP2/II		74.9		
	CCSD(T)/II		75.7		
	experiment[d]		74.1		

[a] Reference 47. [b] Reference 48. [c] Reference 16. [d] Reference 49.

The geometries of the reactants and products involved in the gas-phase reaction 1 and the available experimental data are summarized in Table 1. There is good general agreement in the geometrical parameters with a largest deviation from experiment of 3.6 pm in the bond lengths (for GeH_4 with CCSD(T)/II) and 2° in the bond angles (for SiH_2 with MP2/II). It is

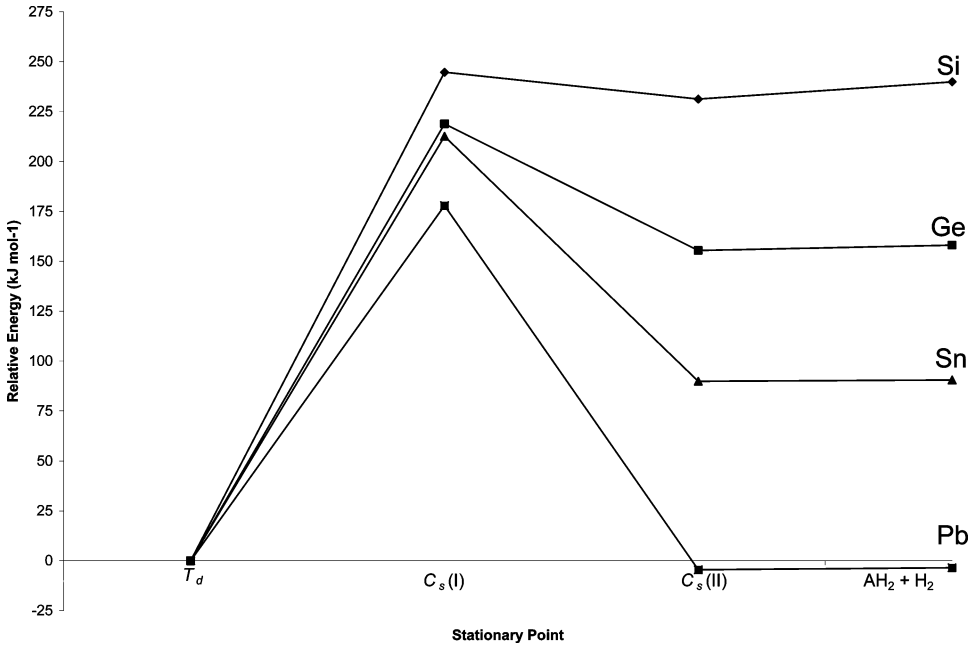

Figure 2. Relative energies obtained with CCSD(T)/II. The values include the scaled ZPE correction.

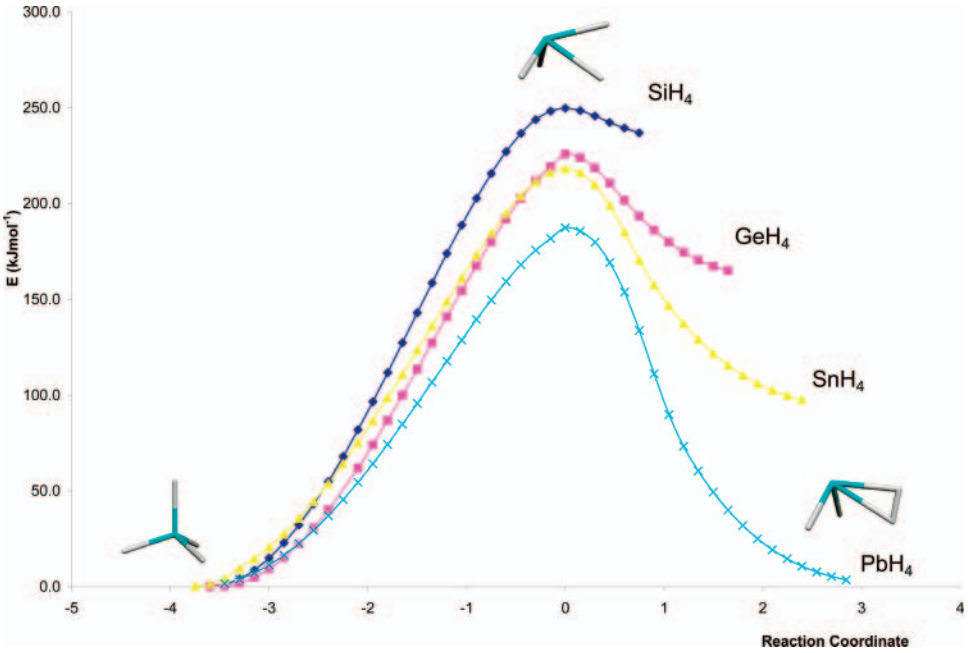

Figure 3. Energy profiles for the dissociation reactions of group 14 hydrides calculated by the IRC method.

TABLE 2: Bond Distances (in pm) and Bond Angles (in deg) for AH_4 Transition States, C_s(I)

A	method	A−H$_1$	A−H$_2$	A−H$_3$	H$_1$−H$_2$	H$_1$−A−H$_2$	H$_3$−A−H$_3$′
Si	B3LYP/I	152.4	165.0	148.6	114.4	42.0	109.7
	MP2/I	151.4	163.0	147.7	114.8	42.7	109.4
	CCSD(T)/I	152.3	164.9	148.4	115.2	42.4	108.7
	B3LYP/II	153.6	165.9	148.6	109.8	40.0	108.8
	B3LYP/III	155.9	173.4	150.8	116.1	40.8	108.8
	MP2/II	153.9	166.3	148.7	109.9	39.9	108.3
	CCSD(T)/II	154.8	168.8	149.6	110.3	39.5	107.8
Ge	B3LYP/I	156.8	172.2	153.9	124.9	44.3	110.5
	MP2/I	154.1	166.7	150.4	118.0	42.9	109.5
	B3LYP/II	158.3	174.0	155.1	124.3	43.6	110.7
	B3LYP/III	158.1	175.5	155.3	128.2	44.8	110.5
	MP2/II	158.8	174.3	155.2	124.7	43.6	110.2
	CCSD(T)/II	159.9	177.7	156.3	125.7	43.3	109.0
Sn	B3LYP/II	174.1	192.2	171.6	135.5	43.1	112.4
	B3LYP/III	174.4	194.0	172.0	136.2	42.9	112.2
	MP2/II	174.4	192.6	171.5	135.0	42.8	112.5
	CCSD(T)/II	175.7	197.3	173.0	136.9	42.6	110.9
Pb	B3LYP/II	175.4	197.5	174.6	152.3	47.8	112.2
	B3LYP/III	176.3	199.4	175.6	148.8	46.2	112.0
	MP2/II	175.7	197.5	174.4	152.9	47.9	112.4
	CCSD(T)/II	177.5	202.5	176.3	156.8	48.2	110.9

important to mention that, even though the scope of the present work is to cover all the elements belonging to group 14, carbon has been excluded because it was the only case where there is no local minimum between the C_s(I) transition state and the dissociation limit, and also because the ground-state multiplicity of CH_2 is a triplet and not a singlet as occurs with the other group 14 dihydrides.

As was mentioned before, for all the group 14 elements considered in this work, a weakly bound intermediate was found between the transition state, C_s(I), and the dissociation limit. The existence of these intermediates suggests that the dissociation reaction of the group 14 tetrahydrides is a two-step process that goes from the tetrahedral structure to the C_s(I) transition state and, before dissociating into AH_2 and H_2, it goes through the C_s(II) intermediate. However, as will be discussed below, the lability of the tin and lead complexes indicates that for these two elements the dissociation of the tetrahydride is a single-step process. The IRC calculations depicted in Figure 3 confirm that these weak molecular complexes are connected to its corresponding transition state.

TABLE 3: Bond Distances (in pm) and Bond Angles (in deg) for the AH_4 Intermediate, C_s(II)′

A	method	A−H$_1$	A−H$_2$	A−H$_3$	H$_1$−H$_2$	H$_1$−A−H$_2$	H$_3$−A−H$_3$′
Si	B3LYP/I	179.1	188.2	151.6	80.2	25.1	94.8
	MP2/I	174.9	181.1	150.5	80.4	26.0	94.9
	CCSD(T)/I	177.5	183.9	151.2	80.3	25.6	94.6
	B3LYP/II	175.4	185.8	151.0	82.2	26.1	96.2
	B3LYP/III	187.2	199.3	153.3	79.7	23.5	93.6
	MP2/II	177.9	186.1	151.2	81.4	25.7	95.3
	CCSD(T)/II	182.2	190.9	152.3	81.2	25.0	94.6
Ge	B3LYP/I	203.6	211.1	159.1	77.3	21.4	92.2
	MP2/I	184.4	190.7	154.6	78.8	24.2	93.2
	CCSD(T)/I	189.6	195.5	156.0	78.5	23.5	92.7
	B3LYP/II	206.0	214.2	160.0	77.9	21.2	92.3
	B3LYP/III	214.9	221.7	161.2	77.2	20.2	91.7
	MP2/II	211.4	216.3	160.0	77.4	20.8	91.7
	CCSD(T)/II	217.8	222.1	161.3	77.7	20.3	91.3
Sn	B3LYP/II	243.3	247.6	178.0	76.3	17.8	91.3
	B3LYP/III	250.9	254.7	179.1	76.1	17.3	90.8
	MP2/II	250.5	251.3	177.7	76.1	17.4	91.1
	CCSD(T)/II	256.5	256.6	179.0	76.6	17.2	90.9
Pb	B3LYP/II	259.5	260.1	183.2	75.9	16.8	90.5
	B3LYP/III	274.7	274.5	184.8	75.6	15.8	90.9
	MP2/II	265.0	262.8	183.1	75.7	16.5	90.1
	CCSD(T)/II	268.6	266.1	184.6	76.4	16.4	90.1

The geometrical parameters of the optimized transition states and intermediates are reported in Tables 2 and 3, respectively. As can be seen, the H$_1$−H$_2$ bond lengths of the leaving hydrogen molecule in the C_s(I) structures increase systematically on going from silicon to lead, indicating that silane has a latter transition state than plumbane (Hammond's postulate).[44] Comparison between the C_s(I) and C_s(II) structures shows that, independently of the methodology, all A−H bond lengths in the intermediate are longer than those in the transition state, and the H$_1$−H$_2$ distances of the most distant hydrogen atoms in the $AH_2\cdots H_2$ complexes are shorter than in the related C_s(I) structure. For silicon and germanium, this distance is larger, by 6 and 2 pm (at CCSD(T)/II), than in H_2. This stretching is not negligible and suggests that important electronic interactions between the AH_2 and H_2 fragments are responsible for the existence of the intermediates. In contrast, the tin and lead complexes have a reduction of this bond length by about 1.0 pm (at CCSD(T)/II), indicating that for these elements, the intermediate is a more labile structure than the silicon and germanium analogues.

TABLE 4: Relatives Energies (in kJ mol^{-1}) with Respect to the T_d Geometries of AH_4, Including the ZPE Correction

A	method	C_s(I)	C_s(II)	AH_2, $C_{2v} + H_2$
Si	B3LYP/I	229.9	208.5	222.2
	MP2/I	241.8	223.0	247.9
	CCSD(T)I	237.0	215.9	238.2
	B3LYP/II	238.4	228.2	244.9
	B3LYP/III	223.8	194.2	202.7
	MP2/II	251.8	240.4	253.9
	CCSD(T)/II	244.7	231.3	239.9
Ge	B3LYP/I	205.4	143.5	149.1
	MP2/I	222.5	189.8	191.2
	B3LYP/II	214.8	155.8	161.1
	B3LYP/III	205.2	128.6	131.7
	MP2/II	227.2	163.6	167.9
	CCSD(T)/II	218.9	155.4	158.1
Sn	B3LYP/II	208.8	89.7	90.0
	B3LYP/III	207.0	79.6	78.8
	MP2/II	225.3	94.7	95.7
	CCSD(T)/II	212.6	89.9	90.5
Pb	B3LYP/II	177.6	−4.6	−5.0
	B3LYP/III	176.4	−2.5	−4.6
	MP2/II	191.5	−5.0	−4.1
	CCSD(T)/II	177.9	−4.5	−3.5

Figure 2 and Table 4 show the energy differences, including the scaled ZPE, between the T_d isomers and the molecular species involved in reaction 3. To discuss the trends, the results corresponding to the CCSD(T)/II calculations will be used, even though other results are closer to the available experimental values. The energies for reaction 1 decrease significantly when one descends in the group: they go from 239.9 kJ mol^{-1} for Si to −3.5 kJ mol^{-1} for Pb. It is worth noting that the calculated value for silicon is in very good agreement with the experimental value reported experimentally by Moffat et al. (231.4 kJ mol^{-1}).[12] Similarly, the relative energies of the transition states decrease from silicon (244.7 kJ mol^{-1}) to lead (177.9 kJ mol^{-1}). For silicon, these energy differences are in excellent agreement with those estimated by using diverse ab initio calculations and with the experimental result (233.9 kJ mol^{-1}).[12] For the insertion reaction of H_2 into silylene, Walch and Dateo stated that "the reaction of SiH_2 with H_2 has no barrier at high level of calculation".[10] However, they did not consider the presence of the C_s(II) intermediate. These complexes are high-lying local minima for Si (231.3 kJ mol^{-1}), Ge (155.4 kJ mol^{-1}), and Sn (89.9 kJ mol^{-1}), but for lead this is the lowest lying isomer (−4.5 kJ mol^{-1}). The energy differences, including ZPE, between the dissociation limit and the intermediates have the following values: 8.6, 2.7, 0.6, and −1.0 kJ mol^{-1}, for Si, Ge, Sn, and Pb, respectively. The small values for silicon and germanium suggest that for these two elements the intermediate is a weakly bounded fluxional structure. For tin, it is marginally stable, and it is definitely undetectable for the case of lead.

To investigate the importance of the scalar relativistic effects in the stationary points of the lead hydrides, additional calculations with a Stuttgart nonrelativistic ECP were done. The scalar relativistic contributions have an important effect in the stability of the C_s(II) intermediate of the lead hydride. Neglecting relativity, the Pb intermediate is 87.4 kJ mol^{-1} above the PbH_4 (T_d) structure but, surprisingly, the inclusion of scalar relativistic effects results in having this intermediate 2.7 kJ mol^{-1} below the T_d moiety. On the other hand, relativity also has an influence in the dissociation barrier of PbH_4 by lowering this energy difference by 40 kJ mol^{-1} with respect to the nonrelativistic calculation, while the activation energy for H_2 insertion, taken as the difference between the C_s(I) transition state and the C_s(II) intermediate, is about 50 kJ mol^{-1} larger when scalar relativistic effects are present. Thus, relativity contributes to enhance the difficulty of inserting dihydrogen to PbH_2 to produce plumbane, and facilitates the dissociation of plumbane into PbH_2 and H_2. The synergy of these two effects explains the difficulty of isolating plumbane: among the group 14 hydrides, plumbane is the case with the smallest barrier to dissociate and the largest to insert H_2 into PbH_2.

IV. Harmonic Frequencies

The results of the vibrational analysis are presented in Table 5. Hitherto, the experimental studies of these systems have not consider explicitly the existence of the C_s(II) intermediates in the decomposition of silane, germane, stannane, and plumbane. This fact is important because, as will be shown in the present section, a pair of bands in the infrared spectra of some of these systems can be assigned to a pair of normal modes coming from the intermediate $AH_2\cdots H_2$ complex.

The infrared spectra for laser-ablated silicon co-deposited with 10% H_2 in neon at 3.5 K for 60 min, reported by Andrews and

TABLE 5: Harmonic Frequencies, ω (in cm^{-1}), and Infrared Intensities, A_i (in km mol^{-1}), Determined with B3LYP/II and Scaled by 0.9806

	Si			Ge			Sn			Pb		
	ω	A_i		ω	A_i		ω	A_i		ω	A_i	
AH_4, T_d	896.0	123	t_2	816.6	132	t_2	703.5	205	t_2	662.4	200	t_2
	896.0	123	t_2	816.6	132	t_2	703.5	205	t_2	662.4	200	t_2
	896.0	123	t_2	816.6	132	t_2	703.5	205	t_2	662.4	200	t_2
	964.4	0	e	899.6	0	E	746.0	0	e	710.5	0	e
	964.4	0	e	899.6	0	E	746.0	0	e	710.5	0	e
	2220.6	0	a_1	2075.0	143	t_2	1869.2	197	a_1	1798.4	0	a_1
	2226.0	115	t_2	2075.0	143	t_2	1869.2	197	t_2	1800.6	254	t_2
	2226.0	115	t_2	2075.0	143	t_2	1869.2	197	t_2	1800.6	254	t_2
	2226.0	115	t_2	2083.3	0	a_1	1885.5	0	t_2	1800.6	254	t_2
AH_4, C_s	542.1	0	a″	340.7	1	a″	199.5	1	a″	102.1	3	a″
	615.0	4	a′	437.0	13	a′	324.0	12	a′	291.5	3	a′
	748.7	6	a′	582.5	19	a′	411.4	30	a′	336.4	52.8	a′
	842.4	7	a″	620.3	0	a″	426.0	0	a″	345.8	0	a″
	981.3	64	a′	898.1	60	a′	698.8	28	a′	609.8	19	a′
	1364.2	60	a′	946.8	27	a′	775.7	74	a′	732.1	51	a′
	2075.2	130	a′	1858.7	265	a′	1669.1	462	a′	1560.9	579	a″
	2081.5	218	a″	1864.5	354	a″	1672.8	374	a″	1562.9	494	a′
	3191.5	142	a′	3807.6	8.8	a′	4059.2	0	a′	4140.2	3	a′
AH_2, C_{2v}	1000.4	74	a_1	912.8	63	a_1	779.2	81	a_1	731.3	52.1	a_1
	2032.3	286	b_2	1845.9	344.8	a_1	1663.5	489	b_2	1561.7	607	b_2
	2033.2	247	a_1	1848.4	395	b_2	1669.4	433.9	a_1	1565.8	541	a_1

Wang,[17] shows two weak unassigned bands in the 2063- and 2095-cm^{-1} regions. The B3LYP/II calculation predicts two scaled frequencies at 2081.5 and 2075.2 cm^{-1} for the C_s(II) complexes.[37] These bands are blue-shifted by 48.3 and 42.9 cm^{-1} with respect to the b_2 and a_1 SiH_2 normal modes, which are almost degenerate. Note that the intensities of these bands are not small and, thus, they can be assigned to the $SiH_2\cdots H_2$ intermediate.

A similar behavior is observed for the germanium hydrides. Wang et al. report a blue site in the neon matrix that disappears on annealing and photolysis at 1867.6 cm^{-1}.[18] They presume that this line can be due to the presence of a $(H_2)GeH_2$ complex. The harmonic analysis of the $GeH_2\cdots H_2$ complex (see Table 5) shows two normal modes located at 1864.5 and 1858.7 cm^{-1}. In this case, the blue shifts are 16.1 and 12.8 cm^{-1}, respectively. Again, from the positions and intensities, these bands can be assigned to the C_s(II) intermediate.

For the tin and lead hydrides, the detection becomes more difficult, not only because the intermediates are less stable with respect to dissociation, as was discussed in the previous section, but also because the normal modes that were used in Si and Ge to identify the intermediates in the infrared spectra are closer to the frequencies coming from the AH_2 species (less than 6 and 3 cm^{-1} for tin and lead, respectively).

For the tin and lead hydrides, Wang and Andrews pointed out that "the blue shoulder which appears on the AH_2 absorption in these experiments is probably due to the $(H_2)AH_2$ complex intermediate in the reaction to form AH_4 product",[16] in full agreement with the results obtained in the present work for silicon and germanium, but due to the coalescence of these two sets of frequencies in tin and lead, their definite identification is more difficult. This fact can be fully appreciated in the simulated spectra depicted in Figure 4.[45]

V. Molecular Orbital Analysis

There has been some controversy regarding the underlying reason for the stability of the intermediate complexes. Thus, to gain further insight into the underlying electronic mechanism that leads to the existence of the C_s(II) complexes, in this section an analysis of the molecular orbitals (MOs) of the chemical structures involved in the thermal dissociation of the group 14 hydrides is presented. For this analysis, the results obtained with the hybrid functional B3LYP and the LANL2DZ+dp ECP were used. Going from left to right in Figure 5, i.e., following the dissociation pathway, the geometrical distortion that accompanies the change from the T_d structure to C_s(I), the transition state, is controlled by the 3a′ MO. From the Mulliken charges presented in Table 6 it can be seen that this distortion, which breaks the highly symmetric tetrahedral geometry, is accompanied by an important flow of electrons from the leaving hydrides (hydrogens H_1 and H_2) to the A atom. The charge of the group 14 atom is reduced considerably: more than twice for silicon and 1.5 times for lead. Following this dissociation pathway, the next step is the formation of the intermediates C_s-(II), which have been identified as molecular complexes. Some of these structures have been described in the literature as donor−acceptor[20] or van der Waals complexes,[6] labeling that underlines the lability of these structures. From the charges reported in Table 6 it is possible to conclude that the transit to these minima on the PES helps to prepare the departure of the hydrogen molecule. Indeed, for all atoms, the total Mulliken charge of the H_2 fragment is positive and very small. Thus, considering the insertion reaction that leads to the formation of the C_s(II) intermediate, there is a charge donation from the entering hydrogen molecule to AH_2. These electrons are taken from the σ_g bonding MO of H_2 to the LUMO ($1b_1$) of the dihydride which is a vacant p orbital of atom A. As soon as the symmetry lowers to C_s, all MOs belonging to the a_1 and b_1 irreducible representations, as well as the σ_g MO of the hydrogen molecule, belong to the a′ irreducible representation of the C_s point group and, consequently, the orbital interactions that lead

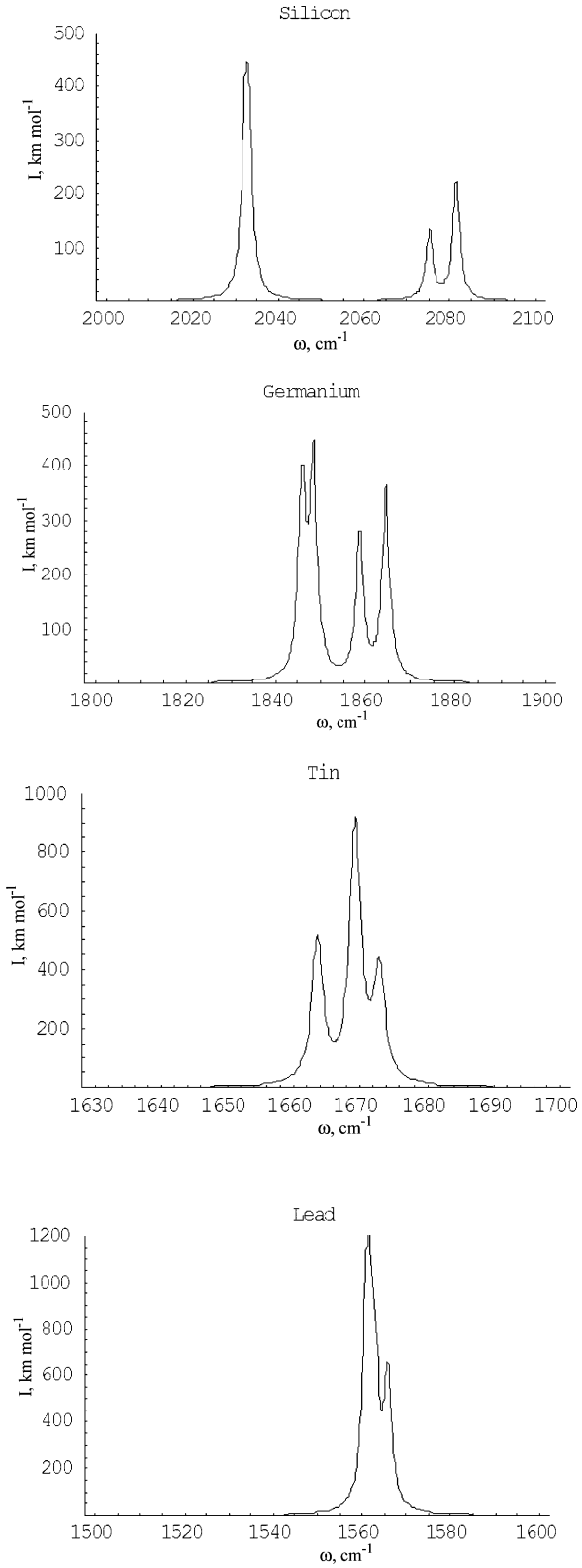

Figure 4. Simulated IR spectra in the regions where one can identify the $AH_2\cdots H_2$ intermediates. The harmonic analysis was done with B3LYP/II.

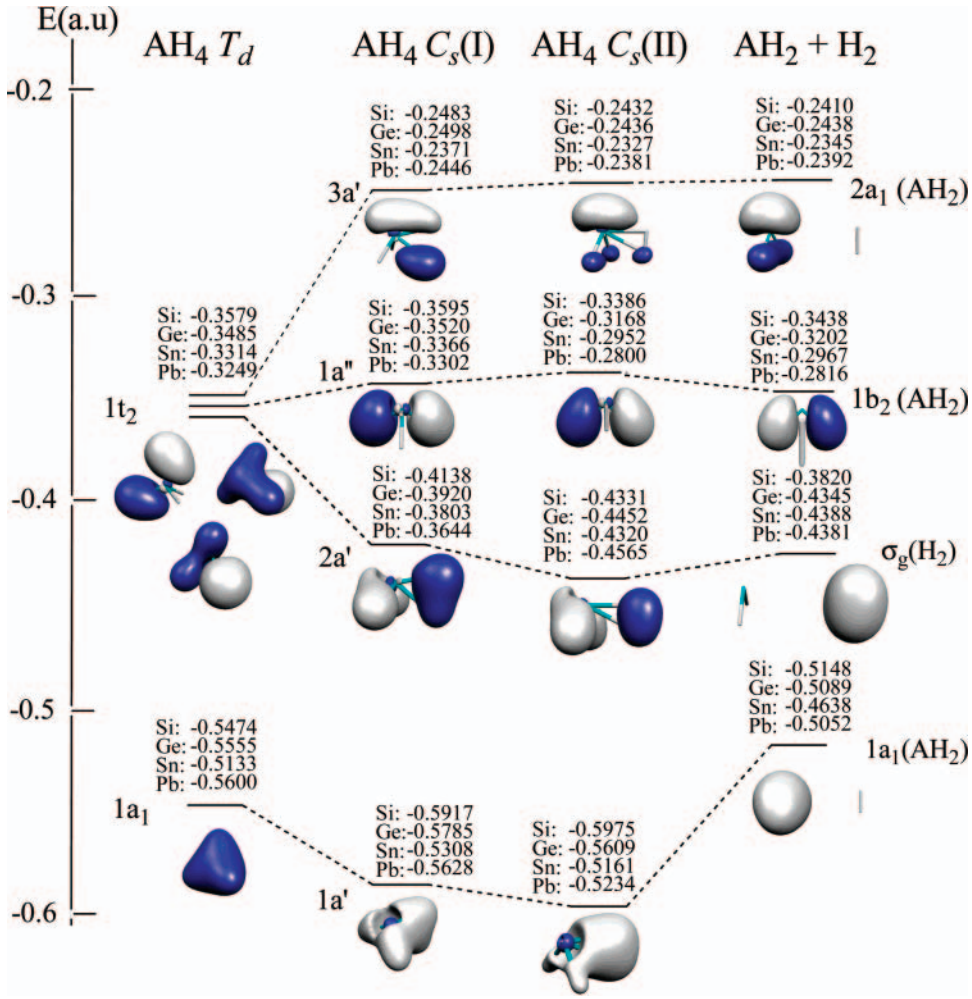

Figure 5. Molecular orbitals of the species involved in the dissociation reaction of group 14 tetrahydrides.

TABLE 6: Mulliken Charges of the Stationary Points of AH_4

		Si	Ge	Sn	Pb
AH_4, T_d	A	0.57	0.55	0.91	0.93
	H	−0.14	−0.14	−0.23	−0.23
AH_4, TS	A	0.27	0.26	0.59	0.62
	H_1	−0.02	−0.02	−0.08	−0.08
	H_2	−0.04	−0.06	−0.14	−0.18
	H_3	−0.11	−0.09	−0.18	−0.18
AH_4, C_s(II)	A	0.22	0.22	0.42	0.49
	H_1	0.01	0.02	0.0	−0.01
	H_2	0.04	0.03	0.03	0.03
	H_3	−0.14	−0.14	−0.23	−0.26
AH_2, C_{2v}	A	0.26	0.27	0.44	0.50
	H	−0.13	−0.14	−0.22	−0.25

to the formation of the intermediate are more complicated. However, from the orbital energies reported in Figure 5, it is possible to conclude that the orbital controlling the formation of the C_s(II) structure is the 2a′. On going from the C_s(I) to the intermediate, one can see from Figure 5 that the HOMOs of all group 14 hydrides remain practically constant along the geometrical distortion. Except for silicon, the absolute changes in the orbital energies are around one order of magnitude larger for 2a′ than for 3a′ (HOMO). The relative variations of these orbital energies are 2−3% for 3a′ and 4−20% for the 2a′ MOs. For these MO energies the silicon compound shows the smallest change. Coming from the hydrogen insertion side, i.e., from the rightmost part of Figure 5 to the left, one also finds that the 2a′ MOs are the ones showing the most important changes during this geometrical transformation. Considering that symmetry does not allow a mixing of the 1a″ MO with the other valence orbitals, one can conclude that the stability of the intermediates can be explained by Walsh's rule, since the MO closest to the HOMO that shows the largest changes along the reaction channel is the 2a′ MO. Summarizing, this MO analysis shows that the insertion of a hydrogen molecule to a group 14 dihydride in the singlet PES is driven by a small electron transfer from the σ_g bonding orbital of H_2 to the LUMO of AH_2 that, due to the lowering (breaking) of symmetry that takes the system to a C_s point group, allows a mixing of the a′ manifold. The 2a′ orbital is the MO with the most relevant change along the reaction path. In compliance with Walsh's rule,[46] and following this insertion route, it is clear that the formation of the transition state is controlled by the 2a′ orbital. Finally, the most prominent change is the passage from the C_s(I) to the T_d structure where there is a very large reshuffling of electron density and, of course, the high symmetry of the tetrahedral species is reflected in the 3-fold degeneracy of the t_2 MOs. That this subtle interplay of orbital interactions is the underlying reason to explain the existence of the C_s(II) intermediates is also supported by the results obtained with the DFT methodology used in the present work. If these complexes were pure van der Waals complexes, one would expect that, at least for some of the group 14 atoms, DFT would not be capable of its detection. Since the observed situation is the converse, one is led to conclude that there must be another mechanism controlling its formation. This mechanism is the small charge transfer plus the orbital interactions described above. Finally, by comparing the sum of the van der Waals

radii of the corresponding group 14 element and hydrogen with the largest A−H distance found in the C_s(II) complexes (see Figure 1), one finds that the former is 80% (Si), 63% (Ge), 31% (Sn), and 20% (Pb) greater than the latter, allowing one to conclude that the weakening of the complexes on descending in the group brings them closer to having a pure van der Waals interaction.

VI. Conclusions

By a careful exploration of the potential energy surface of group 14 hydrides it is shown that the unimolecular thermal dissociation of these compounds goes through an intermediate with C_s symmetry that becomes more unstable as one descends in the group. For silicon and germanium the reaction mechanism is a two-step process, while for tin and lead, the lability of the intermediates suggests that the reaction proceeds as a single-step mechanism. The intermediates found in this work can be used to definitively assign a pair of bands in the infrared spectra of the silicon and germanium hydrides. The instability of the tin and lead complexes and the closeness of the bands in the infrared spectra lead one to conclude that these complexes cannot be unambiguously identified by infrared spectroscopy. It was also found that the large barrier to add a hydrogen molecule to lead dihydride has a relativistic origin. The elucidation of the reaction mechanism for the thermal dissociation of group 14 hydrides can be important in the simulation of chemical vapor deposition.

Acknowledgment. This work was partially funded by Conacyt (projects G34037-E and G32710-E). CGSCA-Cinvestav is gratefully acknowledged for providing computer time in the IBM cluster. G.M. wishes to thank Prof. Seifert and Dr. Heine for their hospitality at the Technische Universität Dresden, where part of this manuscript was prepared.

References and Notes

(1) Jasinski, J. M.; Gates, S. M. *Acc. Chem. Res.* **1991**, *24*, 9−15.
(2) Mahan, A. H.; Carapella, J.; Nelson, B. P.; Crandall, R. S.; Balberg, I. *J. Appl. Phys.* **1991**, *69*, 6728−6730.
(3) Jasinski, J. M.; Meyerson, B. S.; Scott, B. A. *Annu. Rev. Phys. Chem.* **1987**, *38*, 109−140.
(4) Purnell, J. H.; Walsh, R. *Proc. R. Soc. London, Ser. A* **1966**, *293*, 543-&.
(5) Nijhawan, S.; McMurry, P. H.; Swihart, M. T.; Suh, S. M.; Girshick, S. L.; Campbell, S. A.; Brockmann, J. E. *J. Aerosol. Sci.* **2003**, *34*, 691−711.
(6) Gordon, M. S.; Gano, D. R.; Binkley, J. S.; Frisch, M. J. *J. Am. Chem. Soc.* **1986**, *108*, 2191−2195.
(7) Becerra, R.; Boganov, S. E.; Egorov, M. P.; Faustov, V. I.; Nefedov, O. M.; Walsh, R. *Can. J. Chem.* **2000**, *78*, 1428−1433.
(8) Hein, T. A.; Thiel, W.; Lee, T. J. *J. Phys. Chem.* **1993**, *97*, 4381−4385.
(9) Nachtigall, P.; Jordan, K. D.; Smith, A.; Jonsson, H. *J. Chem. Phys.* **1996**, *104*, 148−158.
(10) Walch, S. P.; Dateo, C. E. *J. Phys. Chem. A* **2001**, *105*, 2015−2022.
(11) Hu, S. W.; Wang, Y.; Wang, X. Y.; Chu, T. W.; Liu, X. Q. *J. Phys. Chem. A* **2003**, *107*, 2954−2963.
(12) Moffat, H. K.; Jensen, K. F.; Carr, R. W. *J. Phys. Chem.* **1991**, *95*, 145−154.
(13) Karolczak, J.; Harper, W. W.; Grev, R. S.; Clouthier, D. J. *J. Chem. Phys.* **1995**, *103*, 2839−2849.
(14) Cotton, F. A.; Wilkinson, G.; Murillo, C. A.; Bochmann, M. *Advanced Inorganic Chemistry*, 6th ed.; Wiley: New York, 1999.
(15) Krivtsun, V. M.; Kuritsyn, Y. A.; Snegirev, E. P. *Opt. Spectrosc.* **1999**, *86*, 686−691.
(16) Wang, X. F.; Andrews, L. *J. Am. Chem. Soc.* **2003**, *125*, 6581−6587.
(17) Andrews, L.; Wang, X. F. *J. Phys. Chem. A* **2002**, *106*, 7696−7702.
(18) Wang, X. F.; Andrews, L.; Kushto, G. P. *J. Phys. Chem. A* **2002**, *106*, 5809−5816.
(19) Wang, X. F.; Andrews, L.; Chertihin, G. V.; Souter, P. F. *J. Phys. Chem. A* **2002**, *106*, 6302−6308.
(20) Sosa, C.; Schlegel, H. B. *J. Am. Chem. Soc.* **1984**, *106*, 5847−5852.
(21) Kapp, J.; Schreiner, P. R.; Schleyer, P. v. R. *J. Am. Chem. Soc.* **1996**, *118*, 12154−12158.
(22) Møller, C.; Plesset, M. S. *Phys. Rev.* **1934**, *46*, 618.
(23) Pople, J. A.; Head-Gordon, M.; Raghavachari, K. *J. Chem. Phys.* **1987**, *87*, 5968.
(24) Purvis, G. D.; Bartlett, R. J. *J. Chem. Phys.* **1982**, *76*, 1910.
(25) Scuseria, G. E.; Janssen, C. L.; Schaefer, H. F., III *J. Chem. Phys.* **1988**, *89*, 7382.
(26) Scuseria, G. E.; Schaefer, H. F., III *J. Chem. Phys.* **1989**, *90*, 3700.
(27) Cizek, J. *Adv. Chem. Phys.* **1969**, *14*, 35.
(28) Becke, A. D. *J. Chem. Phys.* **1993**, *98*, 5648−5652.
(29) Lee, C. T.; Yang, W. T.; Parr, R. G. *Phys. Rev. B* **1988**, *37*, 785−789.
(30) Miehlich, B.; Savin, A.; Stoll, H.; Preuss, H. *Chem. Phys. Lett.* **1989**, *157*, 200.
(31) Wadt, W. R.; Hay, P. J. *J. Chem. Phys.* **1985**, *82*, 284−298.
(32) Check, C. E.; Faust, T. O.; Bailey, J. M.; Wright, B. J.; Gilbert, T. M.; Sunderlin, L. S. *J. Phys. Chem. A* **2001**, *105*, 8111−8116.
(33) Bergner, A.; Dolg, M.; Kuchle, W.; Stoll, H.; Preuss, H. *Mol. Phys.* **1993**, *80*, 1431−1441.
(34) Huzinaga, S. A., Jr.; Klobukowski, M.; Radzio-Andzelm, E.; Sakai, Y.; Tatewaki, H. *Gaussian Basis Sets for Molecular Calculations*; Elsevier: Amsterdam, The Netherlands, 1984.
(35) Dunning, T. H.; Hay, P. J. In *Methods of Electronic Structure Theory*; Plenum: New York, 1977.
(36) Dunning, T. H. *J. Chem. Phys.* **1989**, *90*, 1007−1023.
(37) Scott, A. P.; Radom, L. *J. Phys. Chem.* **1996**, *100*, 16502−16513.
(38) Besler, B. H.; Scuseria, G. E.; Scheiner, A. C.; Schaefer, H. F. *J. Chem. Phys.* **1988**, *89*, 360−366.
(39) Fukui, K. *Acc. Chem. Res.* **1981**, *14*, 363−368.
(40) Gonzalez, C.; Schlegel, H. B. *J. Chem. Phys.* **1989**, *90*, 2154.
(41) Frisch, M. J.; Trucks, G. W.; Schlegel, H. B.; Scuseria, G. E.; Robb, M. A.; Cheeseman, J. R.; Zakrzewski, V. G.; Montgomery, J. A.; Stratmann, R. E.; Burant, J. C.; Dapprich, S.; Millan, J. M.; Daniels, A. D.; Kudin, K. N.; Strain, M. C.; Farkas, O.; Tomasi, J.; Barone, V.; Cossi, M.; Cammi, R.; Mennucci, B.; Pomelli, C.; Adamo, C.; Clifford, S.; Ochterski, J.; Petersson, G. A.; Ayala, P. Y.; Cui, Q.; Morokuma, K.; Malick, D. K.; Rabuck, A. D.; Raghavachari, K.; Foresman, J. B.; Cioslowski, J.; Ortiz, J. V.; Baboul, A. G.; Stefanov, B. B.; Liu, G.; Liashenko, A.; Piskorz, P.; Komaromi, I.; Gomperts, R.; Martin, R. L.; Fox, D. J.; Keith, T.; Al-Laham, M. A.; Peng, C. Y.; Nanayakkara, A.; Gonzales, C.; Challacombe, M.; Gill, P. M. W.; Johnson, B.; Chen, W.; Wong, M. W.; Andreas, J. L.; Head-Gordon, M.; Reploge, E. S.; Pople, J. A. *Gaussian 98*, revision A7; Gaussian Inc: Pittsburgh, PA, 1998.
(42) Flükiger, P.; Lüthi, H. P.; Portmann, S.; Weber, J. *MOLEKEL*, 4.3 ed.; Swiss Center for Scientific Computing: Manno, Switzerland, 2000−2002.
(43) Portmann, S.; Lüthi, H. P. *CHIMIA* **2000**, *54*, 766−770.
(44) Hammond, G. S. *J. Am. Chem. Soc.* **1955**, *77*, 334−338.
(45) The IR spectra shown in Figure 4 were calculated by a superposition of loretzian line shapes centered at the values of the corresponding harmonic frequency and with the intensity associated with this normal mode. The width of the line shape is 1 cm^{-1}. No effort was made to include thermal effects.
(46) Albright, T. A.; Burdett, J. K.; Whangbo, M. *Orbital Interactions in Chemistry*; John Wiley & Sons: New York, 1985.
(47) Dyall, K. G.; Taylor, P. R.; Faegri, K.; Partridge, H. *J. Chem. Phys.* **1991**, *95*, 2583−2594.
(48) Dyall, K. G. *J. Chem. Phys.* **1992**, *96*, 1210−1217.
(49) Huber, K. P.; Herzberg, G. Constants of Diatomic Molecules (data prepared by J. W. Gallagher and R. D. Johnson, III). In *NIST Chemistry WebBook*; National Institute of Standards and Technology: Gaithersburg MD, 20899, March 2003.